Article:
Sanderson, Thomas, Black, Conor, Southwell, James et al. (7 more authors) (2020) A Salmochelin S4-inspired Ciprofloxacin Trojan Horse Conjugate. ACS Infectious Diseases. 2532–2541. ISSN 2373-8227

https://doi.org/10.1021/acsinfecdis.0c00568

ACS Infectious Diseases

pubs.acs.org/journal/aidcbc

Article

A Salmochelin S4-Inspired Ciprofloxacin Trojan Horse Conjugate

Thomas J. Sanderson, Conor M. Black, James W. Southwell, Ellis J. Wilde, Apurva Pandey, Reyme Herman, Gavin H. Thomas, Eszter Boros,* Anne-Kathrin Duhme-Klair,* and Anne Routledge*

Cite This: *ACS Infect. Dis.* 2020, 6, 2532−2541

Read Online

ACCESS | Metrics & More | Article Recommendations | Supporting Information

ABSTRACT: A novel ciprofloxacin−siderophore Trojan Horse antimicrobial was prepared by incorporating key design features of salmochelin, a stealth siderophore that evades mammalian siderocalin capture *via* its glycosylated catechol units. Assessment of the antimicrobial activity of the conjugate revealed that attachment of the salmochelin mimic resulted in decreased potency, compared to ciprofloxacin, against two *Escherichia coli* strains, K12 and Nissle 1917, in both iron replete and deplete conditions. This observation could be attributed to a combination of reduced DNA gyrase inhibition, as confirmed by *in vitro* DNA gyrase assays, and reduced bacterial uptake. Uptake was monitored using radiolabeling with iron-mimetic $^{67}Ga^{3+}$, which revealed limited cellular uptake in *E. coli* K12. In contrast, previously reported staphyloferrin-based conjugates displayed a measurable uptake in analogous $^{67}Ga^{3+}$ labeling studies. These results suggest that, in the design of Trojan Horse antimicrobials, the choice of siderophore and the nature and length of the linker remain a significant challenge.

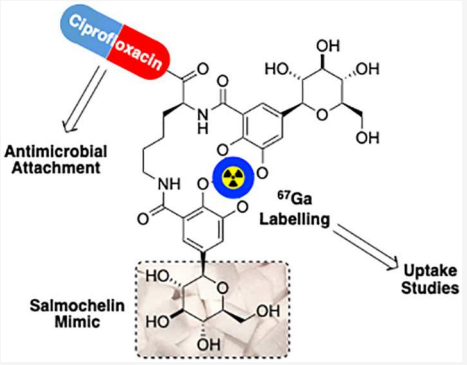

KEYWORDS: *siderophores, antibiotics, drug design, radiolabeling, bioinorganic chemistry*

The problem of antimicrobial resistance has reached a critical level, and authorities now believe humankind is entering a post-antibiotic era where minor infections and routine medical procedures will become major morbidity threats.[1−4] New strategies in the form of new antibiotic targets or modification of current antibiotics to bypass resistance mechanisms are urgently needed.[4−8] One approach is a Trojan Horse delivery strategy that targets outer membrane barrier permeability resistance[9−13] by utilizing bacterial iron transport, mediated by siderophores, to promote active antibiotic uptake; a number of examples can be found in the literature.[14−20] This strategy has been met with some success, with a number of siderophore−drug conjugates entering clinical trials.[4,21−23] One example, cefiderocol (Fetroja, Figure 1), was recently approved by the U.S. Food and Drug Administration (FDA) for treatment of complicated urinary tract infections (cUTIs).[24]

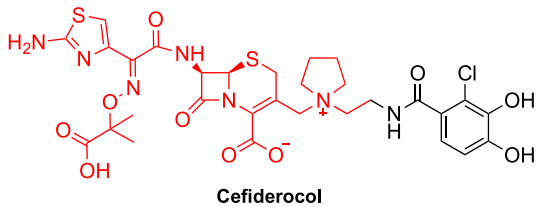

Figure 1. Structure of FDA-approved Trojan Horse antibiotic cefiderocol (antibiotic unit highlighted in red).

Salmochelin siderophores, identified in 2003,[25] are a family of siderophores consisting of glycosylated variants of the high-Fe^{3+}-affinity tris-catecholate siderophore enterobactin produced by many of the Enterobacteriaceae.[26] The family derives from the diglycosylated hexadentate salmochelin S4 (Figure 2) and includes a series of di- and monoglycosylated hydrolysis products.[27] Salmochelins are biosynthesized by a range of bacteria, including *Salmonella* spp. and various pathogenic *E. coli* strains.[25,28,29]

The salmochelins belong to a class of stealth siderophores, which maintain their role in bacterial iron acquisition while evading the host innate immune response.[30] As a response to an invading pathogen, the mammalian host secretes immunoprotein siderocalin to capture Fe^{3+}-loaded catecholate-based siderophores.[31,32] The glycosyl units in the salmochelins prevent siderocalin binding, thus allowing the siderophores to avoid capture. The ability to produce and utilize salmochelins relies on the *iroA* gene cluster,[30] which encodes the enzymes responsible for the glycosylation of catechol units, the secretion of the biosynthesized salmochelins, the uptake of their Fe^{3+} complexes, and finally, the

Received: August 6, 2020
Published: August 11, 2020

https://dx.doi.org/10.1021/acsinfecdis.0c00568
ACS Infect. Dis. 2020, 6, 2532−2541

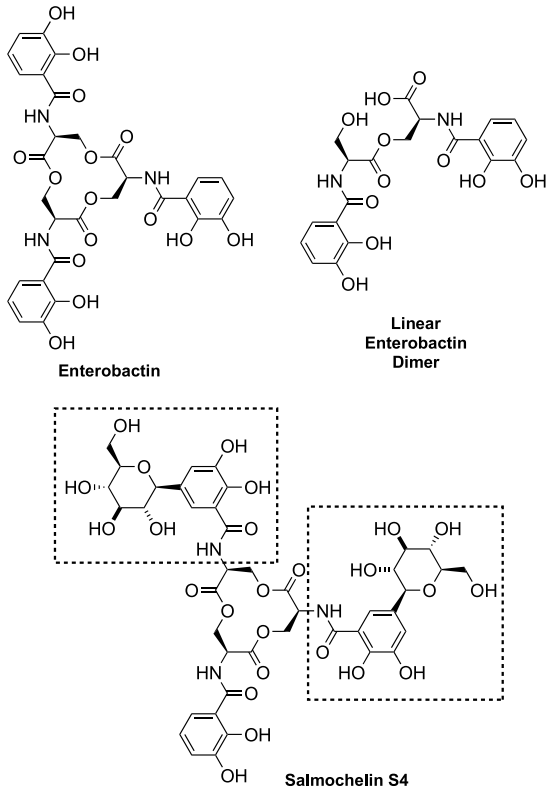

Figure 2. Chemical structures of siderophores: enterobactin, linear enterobactin dimer, and salmochelin S4, with characteristic glycosylated catechol units of salmochelin S4 highlighted.

hydrolysis of both the apo- and Fe^{3+}-bound siderophores.[33] While the salmochelin uptake mechanism[34,35] is thought to share similarities with that of enterobactin,[18,36−38] the enterobactin receptor protein FepA, found in all *E. coli*, is unable to mediate significant uptake of salmochelin S4, whereas the outer membrane receptor protein IroN, which is expressed only in strains that harbor *iroA*, allows uptake of both salmochelin S4 and enterobactin (see Figure 3).[25] This key difference means that the presence of the *iroA* gene cluster is considered a virulence factor.

The production of siderocalin by the host may limit the application of catecholate siderophores in Trojan Horse antimicrobials, unless the siderophore component is structurally modified to evade the immune response, while maintaining high affinity for Fe^{3+}. The use of salmochelin-based siderophore components offers the opportunity of specifically targeting bacteria that express the salmochelin transport machinery, while minimizing disruptions to the host microbiome. This approach has been successfully demonstrated by Nolan et al. with the chemoenzymatic synthesis of glucosylated enterobactin−β-lactam conjugates (Figure 4).[39]

Figure 3. Simplified schematic representation of the outer membrane receptor proteins involved in Fe^{3+}-siderophore uptake in all *E. coli* (left) and pathogenic *E. coli* capable of producing salmochelin (right).

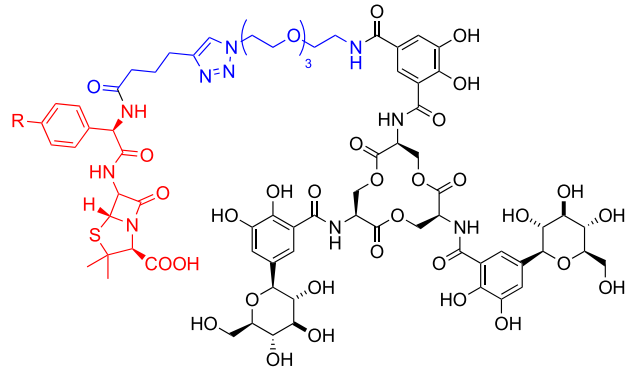

Figure 4. Salmochelin−β lactam conjugate designed and synthesized by Nolan and co-workers (antibiotic component in red, chemical linker in blue, and siderophore in black).

As part of our wider investigation into fluoroquinolone siderophore conjugates,[40−42] we herein report the design and synthesis of a first generation ciprofloxacin−salmochelin S4 inspired Trojan Horse antimicrobial **1** (Figure 5), designed to evade the mammalian siderocalin immune response and to selectively target bacteria expressing salmochelin transport machinery.

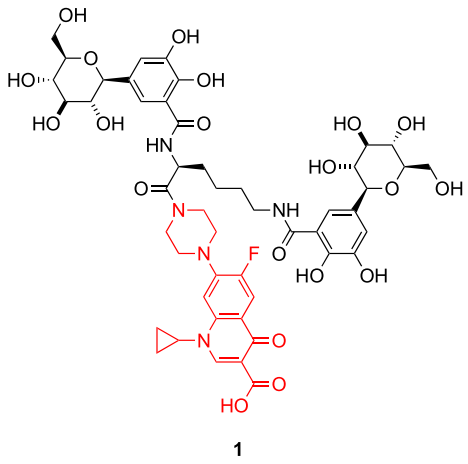

1

Figure 5. Salmochelin S4-inspired Trojan Horse antimicrobial.

RESULTS AND DISCUSSION

Design and Synthesis. In our approach to the design of a first generation salmochelin S4-inspired ciprofloxacin conjugate, the salmochelin S4 structure was simplified to a synthetically accessible structure, comprising an aliphatic link based on L-lysine between the catechol units and a reduction of siderophore denticity from hexadentate to tetradentate. L-Lysine was utilized to mimic the chirality and exact length of the backbone between the catechol moieties in salmochelin S4

https://dx.doi.org/10.1021/acsinfecdis.0c00568
ACS Infect. Dis. 2020, 6, 2532−2541

in a hydrolytically stable manner; the ester backbone in salmochelin is prone to hydrolysis under physiological conditions. The tetradentate siderophore mimic allows for improved synthetic tractability compared to when the full triserine scaffold of salmochelin S4 is used. The carboxylic acid group of the lysine moiety provides an attachment point for the antimicrobial. It was shown previously that tetradentate, diamine-linked bis(catecholates) can function as siderophore components in Trojan Horse antimicrobials, which were shown to penetrate at least the outer membrane of Gram-negative bacteria, including *E. coli*.[43,44]

We anticipated compound **1** to possess similar iron-binding properties to the tetradentate linear enterobactin dimer[45] (Figure 2) and a previously described salmochelin S1 mimic,[46] as both feature similar 2,3-dihydroxybenzamide iron-chelating moieties attached to a 5-atomic backbone. We have previously investigated the Fe^{3+} coordination chemistry of these two tetradentate bis(catecholates) by using both UV−vis and CD spectroscopy and observed rapidly equilibrating mixtures of 1:1 and 2:3 complexes, both monomers and dimers. In compound **1**, however, the deprotonated carboxylic acid and adjacent carbonyl donor of the ciprofloxacin moiety could act as an additional third iron chelating unit and hence affect the iron-binding properties.[47,48]

The C5-β-glycosyl-2,3-dihydroxybenzoyl units of salmochelin S4 (highlighted in Figure 2) were amalgamated into the design but connected *via* $N_\alpha N_\varepsilon$ of L-lysine, with the *C*-terminus providing an appropriate handle for attachment of the parent antibiotic, ciprofloxacin. Suitably functionalized catechol units were synthesized using previously described methodologies. Commercially available methyl 3-methoxysalicylate **2** was iodinated with iodine monochloride[49] and then demethylated. This was followed by benzylation of the free phenolic hydroxyl groups to give **3**. Acetyl-protected β-glucose was installed *via* nickel-promoted Negishi coupling using an adapted literature procedure[50,51] to give aryl-*C*-glucoside **4**. The glucosyl acetyl protecting groups of **4** were substituted with benzyl ethers, resulting in the formation of two compounds **5** and **6**, which were combined and then hydrolyzed to give the free carboxylic acid **7** (Scheme 1).[50]

In order to furnish a suitably functionalized antimicrobial to allow the salmochelin analogue to be constructed, L-lysine-appended ciprofloxacin **10** was synthesized as shown in Scheme 2. Commercially available ciprofloxacin was converted into its benzoyl ester **8** *via* a transient *t*-butyloxycarbonyl nitrogen protection/deprotection strategy. It was then coupled to $N_\alpha N_\varepsilon$-diboc-L-lysine *via* EDC-mediated amide formation to give **9**.

Deprotection of the lysine-associated protecting groups yielded **10**. Lysine functionalized ciprofloxacin was coupled with glucosylated catechol **7** to give benzyl-protected salmochelin-inspired conjugate **11**. Global debenzylation with Pearlman's catalyst[52] furnished salmochelin-inspired ciprofloxacin conjugate **1** in a moderate yield. Experimental details are provided in the Supporting Information.

Fe^{3+} Complex Formation. The Fe^{3+} complex of **1** (1:1 ratio) was prepared by combining equimolar amounts of **1**, dissolved in DMSO, and $FeCl_3$ hexahydrate, dissolved in water. The solvents were removed *in vacuo*, and the resulting residue was taken up in a volatile buffer (ammonium acetate) to enable the species formed at pH 7.4 to be examined by native ion mass spectrometry (experimental details are provided in the Supporting Information). Complexation was confirmed by

Scheme 1[a]

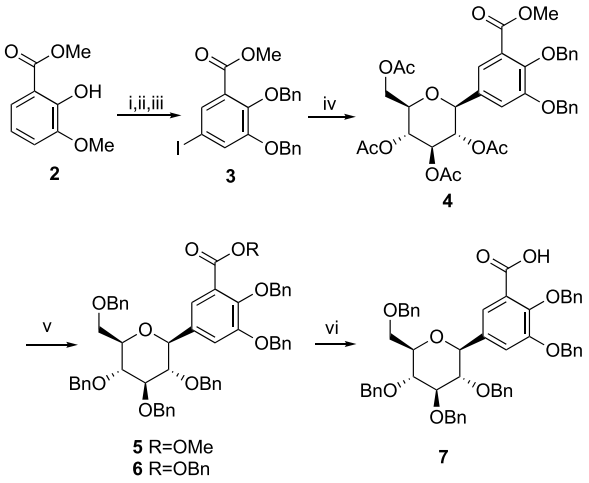

[a](i) $AgNO_3$, ICl, pyridine, $CHCl_3$, 68%; (ii) (1) BBr_3, CH_2Cl_2, (2) H_2SO_4, CH_3OH, 91%; (iii) benzyl bromide, NaI, DMF, 72%; (iv) 1-bromo-α-D-glucose tetraacetate, Zn, LiCl, $Ni(COD)_2$, ^{t}BuTerpy, DMF, 63%; (v) (1) Na_2CO_3, MeOH, (2) benzyl bromide, NaH, Bu_4NI, DMF, **5** + **6** 74%; (vi) NaOH, THF/MeOH (3:1), 87%.

UV−vis spectroscopy (Figure S1). The observed λ_{max} of the ligand-to-metal charge transfer band at 544 nm is consistent with the prevalence of a chromophore in which two catecholate units are coordinated to Fe^{3+}, i.e., an equimolar Fe^{3+}-to-**1** ratio.[46]

Interestingly, the negative ion ESI mass spectrum showed evidence for the formation of both 1:1 and 2:2 species, the latter consisting of two Fe^{3+} cations and two $\mathbf{1}^{5-}$ ligands (Scheme S1). The most abundant ions were observed at m/z 553.1336, 583.1437, 737.8462, and 1107.2695. On the basis of their isotope patterns and charges, these peaks could be assigned to the acetate adduct of the monomeric species $[Fe^{3+}L^{5-} + \text{acetate}^- + H^+]^{2-}$, and the dimeric species $[(Fe^{3+}L^{5-})_2]^{4-}$, $[(Fe^{3+}L^{5-})_2 + H^+]^{3-}$ and $[(Fe^{3+}L^{5-})_2 + 2H^+]^{2-}$ (Figure S2). The equilibrium shifts slowly from the monomeric toward dimeric species over the course of several days (Figure S2a−c).

The composition of these ions suggests that the acetate in the 1:1 species and the carboxylate and keto O-donors of ciprofloxacin in the 2:2 species may be recruited to complete the 6-fold coordination sphere of the iron center. Due to the rigid nature of ciprofloxacin, its O-donor atoms can only coordinate to an adjacent iron center, and this may trigger dimer formation. In addition, H-bonding interactions with the glucose unit on the siderophore may support dimer formation.

In addition, a solution containing Fe^{3+} and conjugate **1** in a 2:3 ratio was prepared in an analogous way. The λ_{max} of the ligand-to-metal charge transfer band in the UV−vis spectrum did not shift significantly (Figure S1), and the most abundant ions observed in the negative ion ESI mass spectrum were those assigned to 1:1 and 2:2 species, as above, plus free ligand (conjugate **1**). The formation of a 2:3 complex (Scheme S1) was not apparent (Figure S3). This suggests that the coordination of a third ligand is not favored in this case, potentially due to steric hindrance or competitive binding of the acetate or keto and/or carboxylate O-donors of the ciprofloxacin unit.

Antibacterial Activity Testing. The antibacterial activity of both **1** and the parent drug ciprofloxacin was tested against

https://dx.doi.org/10.1021/acsinfecdis.0c00568
ACS Infect. Dis. 2020, 6, 2532−2541

Scheme 2[a]

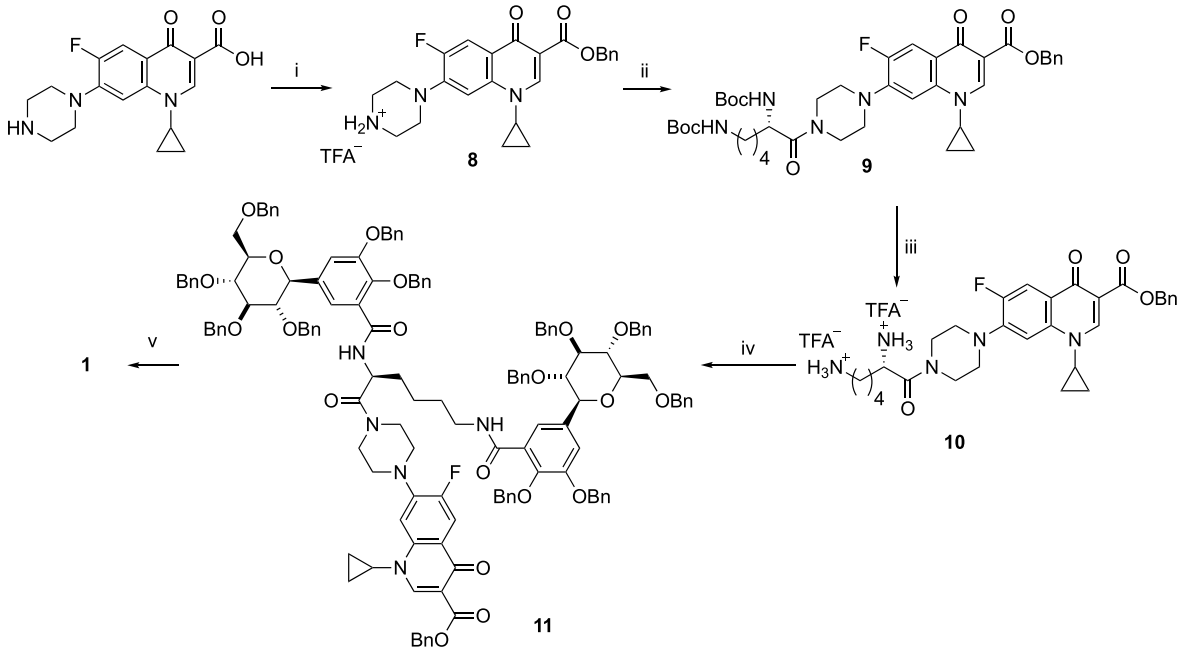

[a](i) (1) Boc_2O, NaOH, 1,4-dioxane, H_2O, (2) benzyl bromide, Cs_2CO_3, DMF, (3) TFA, CH_2Cl_2, 51%; (ii) N_α,N_ε-Boc-lysine, EDC·HCl, HOBt·H_2O, DIPEA, DMF, 55%; (iii) TFA, CH_2Cl_2, 100%; (iv) **7**, EDC·HCl, HOBt·H_2O, DIPEA, DMF, 42%; (v) $Pd(OH)_2$/C, H_2, MeOH/EtOAc (1:1), 45%.

two bacterial strains: (1) *E. coli* K12 (BW25113), a common laboratory strain that does not express IroN, the outer membrane receptor protein required for active salmochelin uptake,[25] and (2) *E. coli* Nissle 1917, a probiotic strain that expresses IroN and is able to utilize salmochelin.[29] In addition to serving as a negative control, the K12 strain was investigated to confirm that nonpathogenic bacterial strains that are unable to utilize salmochelin remain unaffected. The size of **1** renders it unlikely to be taken up passively *via* porins, OmpF or OmpC.[53−57] OmpF is considered the main uptake pathway for ciprofloxacin but has a molecular weight limit of around 600 Da.[58] In the absence of active transport or porin-mediated uptake, passive diffusion across the outer membrane is a possibility; this has been suggested to occur for ciprofloxacin, although to a much lesser degree than uptake *via* porins.[59] However, it is unlikely that **1**, with a projected polar surface area of 401 Å,[60] would display a similar capacity as ciprofloxacin for passive diffusion, with a corresponding approximated polar surface area of 82 Å, in its zwitterionic form; a high polar surface area correlates strongly with decreased membrane permeability.[61]

It was hoped that the presence of the salmochelin transport machinery in Nissle 1917 would support active uptake of the Fe^{3+} complex of **1** and hence increase its antibacterial activity, thereby allowing the selective targeting of this strain.

The antibacterial activity assays were carried out in MOPS acetate minimal media,[62] either in the presence of 100 μM Fe^{3+} (iron replete conditions) or with no added Fe^{3+} (iron deplete conditions, <18 pM Fe). Details of the composition and iron content of the media are provided in the Supporting Information.

As expected, in *E. coli* K12 (BW25113), which lacks the IroN transporter, **1** demonstrated a much lower antibacterial activity than ciprofloxacin under both iron replete and iron deplete conditions. Disappointingly, when the activity was tested against Nissle 1917, capable of expressing IroN, a similar lack of activity of **1** was observed, suggesting that active uptake of **1** is not taking place (Table 1). This observation led to a further investigation of factors limiting uptake/activity (*vide infra*).

Table 1. MIC Values of Conjugate 1 and Ciprofloxacin (cipro) Determined in Acetate/MOPS Minimal Media under Iron Replete (100 μM Fe^{3+}) and Deplete (<18 pM Fe) Conditions

	E. coli K12 (BW25113)		*E. coli* Nissle 1917	
	Fe replete (μM)	Fe deplete (μM)	Fe replete (μM)	Fe deplete (μM)
1	>100	75	>100	100
cipro	1	1	0.1	8

Antibacterial Activity vs *E. coli* K12 (BW25113). Conjugate **1** was added to the growth media at varying concentrations (0−100 μM, Figure 6). At higher concentrations of **1** in iron replete conditions, immediate Fe^{3+}-chelation was evident by the emergence of a characteristic purple color due to Fe^{3+}−siderophore complex formation.[45] Due to the significant absorbance of these complexes at 600 nm, the optical density of the cell cultures is displayed at 800 nm (OD_{800}). As expected, at plateaued bacterial growth (after 48 h) and in the absence of antimicrobial agents, the bacterial cell density obtained in Fe^{3+} replete media was more than twice as high as that obtained under Fe^{3+} limitation (Figures 6 and S6).

In iron replete media, ciprofloxacin, the parent antimicrobial of **1**, was active at low concentrations between 0.1 and 1 μM (Figure 7a), while **1** only showed growth suppression once the concentration started to approach that of Fe^{3+} in the growth medium (>75 μM). In iron deplete conditions, a clear growth

https://dx.doi.org/10.1021/acsinfecdis.0c00568
ACS Infect. Dis. 2020, 6, 2532−2541

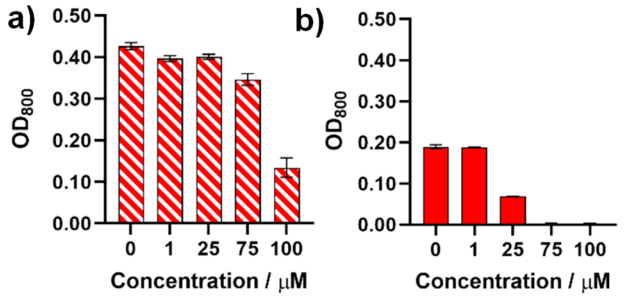

Figure 6. *E. coli* K12 (BW25113) growth in minimal media (MOPS acetate) in the presence of **1** at t = 48 h in (a) iron replete (striped bars) and (b) iron deplete (solid bars) conditions.

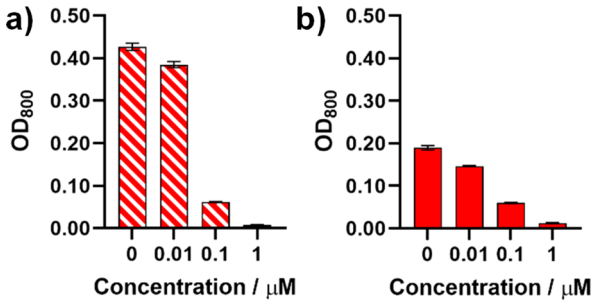

Figure 7. *E. coli* K12 (BW25113) growth in minimal media (MOPS acetate) in the presence of ciprofloxacin at t = 48 h in (a) iron replete (striped bars) and (b) iron deplete (solid bars) conditions.

inhibitory effect was already observed at a 25 μM concentration of **1**. While the latter might be an indication of salmochelin-mediated uptake of **1**, the attenuation of bacterial growth may also be attributed to the competition of **1** with native siderophores for the more limited Fe^{3+} resource, starving the cells of the vital nutrient. Again, the antibacterial activity of **1** was much lower than that of the parent antibiotic ciprofloxacin (~75×, Figure 7b). Hence, to further explore the relationship between siderophore-mediated Fe^{3+} uptake and the antibacterial activity of **1**, a radiolabeling study with the Fe^{3+}-mimetic $^{67}Ga^{3+}$ was undertaken.

^{67}Ga-Radiolabeling and Bacterial Uptake. Hexadentate siderophores exhibit exceptionally high affinity for both Fe^{3+} and the nonredox active, Fe^{3+}-mimetic Ga^{3+} ($K_D > 10^{-30}$ M).[63] Functionalized Ga^{3+} and Fe^{3+} siderophore complexes are both efficiently recognized by bacterial siderophore membrane transporters, indicating that bacteria cannot distinguish the trivalent ions at the time of siderophore-mediated entry. Ga^{3+} represents an ideal surrogate to study the behavior of Fe^{3+} complex species.[64,65] Commercial availability of two radioactive imaging isotopes of Ga^{3+}, ^{68}Ga ($t_{1/2}$ = 1.1 h), a positron emission tomography (PET) imaging isotope, and ^{67}Ga ($t_{1/2}$ = 3.3 d), a longer lived isotope utilized for single photon emission computed tomography (SPECT), provides opportunities to study the stability and pharmacokinetics of Ga–siderophore complexes *in vitro* and *in vivo*. Indeed, this approach has already been explored for the imaging of fungal infections in rats, taking advantage of the siderophore-mediated uptake of ^{68}Ga in fungi such as *A. fumigatus*,[66] as well as the assessment of a novel desferrichrome-based conjugate that exhibited enhanced potency in Gram-positive and Gram-negative strains.[19]

Here, we elected to use ^{67}Ga, as the longer half-life of this isotope permits extensive long-term stability and internalization studies. It has been shown that ^{67}Ga-labeled deferoxamine (DFO) retains active uptake *via* bacterial Fe^{3+}-transport in *S. aureus* with DFO acting as a xenosiderophore.[67,68] In order to synthesize ^{67}Ga-**1**, we first transformed ^{67}Ga-citrate to $GaCl_3$ and monitored the radiolabeling of **1** by radio-HPLC.[19] Complexation proceeds quickly with quantitative yield, producing an apparent molar activity of 90 nmol/MBq. In order to probe if the ^{67}Ga-**1** was sufficiently inert for subsequent uptake experiments, we monitored complex inertness in LB broth over the course of 2 h, during which no significant dechelation was observed. Next, we assessed the time-dependent bacterial uptake of ^{67}Ga-**1** in *E. coli* K12 (MG1655) in iron replete LB over 2 h. The percentage of internalized ^{67}Ga-**1** was <10% of the total ^{67}Ga and comparable to the uptake of a ^{67}Ga-citrate control. The results in iron deplete LB media were similar, with <10% internalization, comparable to that seen with ^{67}Ga-citrate (Figure 8).

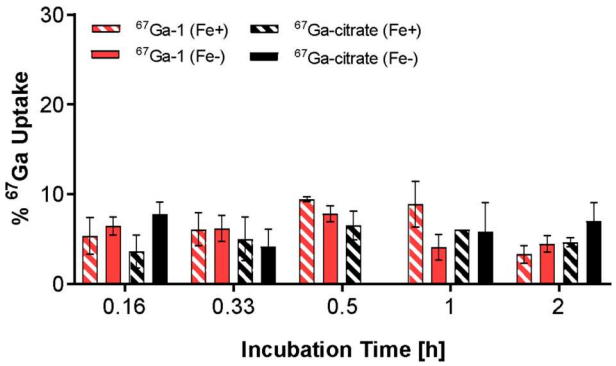

Figure 8. Time-dependent, radiochemical bacterial uptake studies in *E. coli* K12 (MG1655) of ^{67}Ga-**1** in iron replete (striped bars) and iron deplete (solid bars) media. Error bars calculated as standard deviation of n = 5.

To confirm if this measured uptake mirrored low transport into bacteria, with the resultant absence of activity, the study was expanded to assess three compounds previously reported by us, staphyloferrin A-inspired conjugates **12**, **13**, and **14** (Figure 9).[40] These conjugates retain and mirror the original

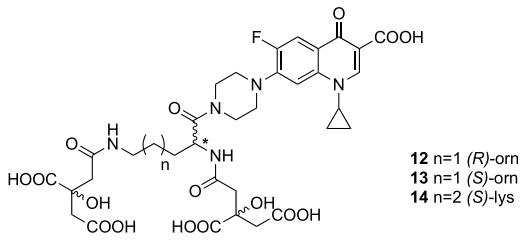

Figure 9. Structures of staphyloferrin A–ciprofloxacin conjugates **12**–**14**.

siderophore structure more closely and provide a 6-coordinate ligand environment for corresponding Fe^{3+} and Ga^{3+} complexes. These compounds showed activity against *E. coli* NCTC10418 and some inhibition of DNA gyrase *in vitro*, albeit at a lower level than the parent ciprofloxacin.[41] All three compounds have an estimated polar surface area of 329 Å when fully protonated. In analogy to ^{67}Ga-**1**, ^{67}Ga-**12**, ^{67}Ga-**13**, and ^{67}Ga-**14** were synthesized under identical conditions.

https://dx.doi.org/10.1021/acsinfecdis.0c00568
ACS Infect. Dis. 2020, 6, 2532–2541

The radiolabeled complexes were less stable than ^{67}Ga-**1** in both iron replete and iron deplete LB broth, exhibiting the percentage of intact radiochemical complexes ranging from ^{67}Ga-**14** (70%) to ^{67}Ga-**12** (60%) and ^{67}Ga-**13** (50%). No further trans-chelation was observed after 9 h, indicating that a relative equilibrium state is reached. In iron deplete LB broth, complex stability was marginally lower but again was maintained over 9 h.

To assess relative complex inertness in comparison with the 6-coordinate chelator ethylenediamine-tetraacetate (EDTA), the radiochemical gallium complexes were challenged with a 10-fold excess with respect to conjugate concentration. Complex inertness was monitored using radio-HPLC. After 2 h, the relative inertness can be ranked as follows: ^{67}Ga-**14** > ^{67}Ga-**12** > ^{67}Ga-**13** > ^{67}Ga-**1** (Figure S11). This result indicates that, in the presence of a six-coordinate, competing chelator, the trans-chelation from a 4-coordinate donor such as **1** occurs rapidly; the 6-coordinate, staphyloferrin-based conjugates provide a more inert coordination environment, with the lysine-derived structure, ^{67}Ga-**14**, showing the best stability in this challenge assay.

Uptake experiments in *E. coli* K12 (MG1655) in both iron replete and deplete LB broth were assessed in comparison with ^{67}Ga-**1**. Although still low (up to 14.7% after 0.33 h for ^{67}Ga-**13**, Figure 10), the uptake of all three conjugates was higher

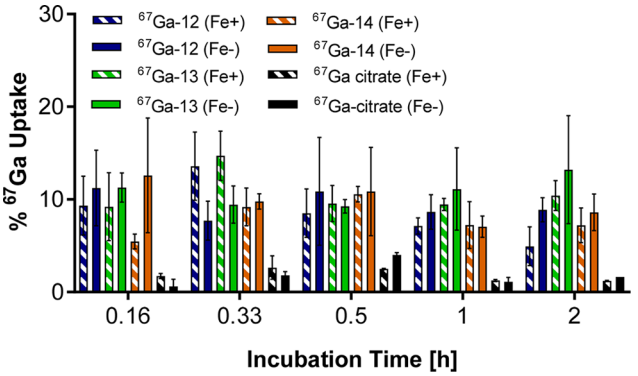

Figure 10. Time-dependent, radiochemical bacterial uptake studies in *E. coli* K12 (MG1655) of ^{67}Ga-staphyloferrin conjugates **12**−**14** in iron replete (striped bars) and iron deplete (solid bars) media. Error bars calculated as standard deviation of $n = 5$.

than that observed with the ^{67}Ga-citrate control and marginally higher than that observed with ^{67}Ga-**1**, suggesting a very modest degree of translocation through bacterial cell membranes, corroborating antibacterial activity results obtained in previous work.[40−42]

Antibacterial Activity vs *E. coli* Nissle 1917. The antibacterial activities of **1** and ciprofloxacin were also assessed against a strain of *E. coli* capable of producing and transporting salmochelin, *E. coli* Nissle 1917. The probiotic Nissle 1917 shares many characteristics with uropathogenic *E. coli* strains, including the ability to produce several siderophores, specifically salmochelin, enterobactin, yersiniabactin, and aerobactin, to be able to adapt to environmental challenges.[29] It was hoped that the presence of the salmochelin transport machinery, including the outer membrane transporter IroN,[25] would increase the bacterial uptake and hence antibacterial activity of **1** in Nissle 1917.

However, the antimicrobial activity of **1** was found to be similar to that observed with the K12 strain. In iron replete media, clear growth inhibition was only seen at 100 μM concentrations and above, when the concentration of **1** reached the 100 μM concentration of Fe^{3+} (Figure 11a).

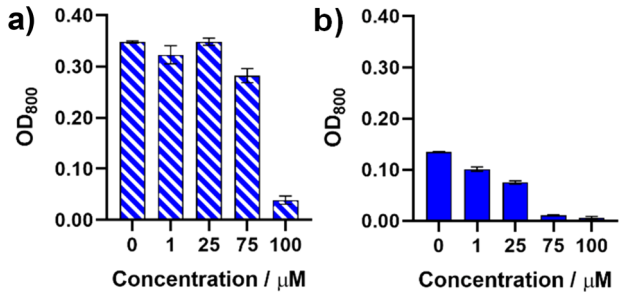

Figure 11. *E. coli* Nissle 1917 growth in minimal media (MOPS Acetate) in the presence of **1** at $t = 48$ h in (a) iron replete (striped bars) and (b) iron deplete (solid bars) conditions.

This suggests that, under these conditions, the sequestration of Fe^{3+} by the siderophore unit of **1** becomes so significant that it deprives the growth medium of this vital nutrient. The fact that ciprofloxacin already suppresses growth at ∼1000× lower concentrations (0.1 μM, Figure 12a) is consistent with a lack of bacterial uptake of **1**.

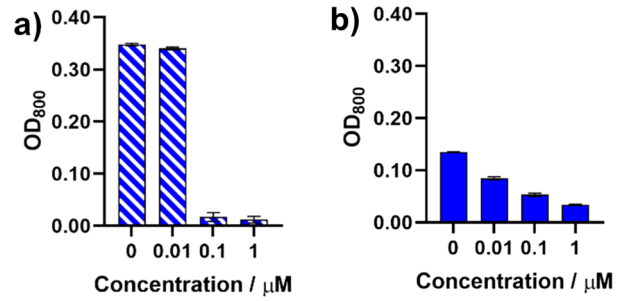

Figure 12. *E. coli* Nissle 1917 growth in minimal media (MOPS acetate) in the presence of ciprofloxacin at $t = 48$ h in (a) iron replete (striped bars) and (b) iron deplete (filled bars) conditions.

In iron deplete media, a slight growth inhibitory effect is already evident at a 1 μM concentration of **1** (Figure 11b). This observation is consistent with both a fiercer competition between the siderophore unit of **1** and native siderophores for the small amount of Fe^{3+} available in the deplete medium and the siderophore-mediated uptake of **1**. However, if active uptake is occurring, the lower activity of **1** compared to that of ciprofloxacin (Figure 12b) suggests that it is insufficient to compensate for the decrease in uptake of the antimicrobial *via* porins and passive diffusion caused by attachment of the salmochelin unit in **1**, even though the expression of high-affinity siderophore transport proteins, such as IroN, should be upregulated under Fe^{3+} limited conditions.[69] The observation that the activity of **1** vs *E. coli* Nissle 1917 is significantly lower than that of its parent drug ciprofloxacin led us to consider poor binding to the drug target DNA gyrase as an additional possible reason for the observed reduction in potency.

Gyrase Inhibition Assay. A key factor in the antimicrobial activity of ciprofloxacin conjugates is their continued ability to inhibit DNA gyrase, the cytoplasmic drug target of ciprofloxacin. In order to investigate the impact of

https://dx.doi.org/10.1021/acsinfecdis.0c00568
ACS Infect. Dis. 2020, 6, 2532−2541

salmochelin-inspired siderophore conjugation on the ability of ciprofloxacin to inhibit gyrase, **1** was evaluated in an *in vitro* assay using a commercial DNA gyrase supercoiling assay. Initially, **1** was studied over a range of concentrations (0.5−20 μM) and no inhibition of gyrase activity was observed, as indicated by no reduction in the presence of supercoiled DNA plasmids on agarose gels (Figure 13). Inhibition of the

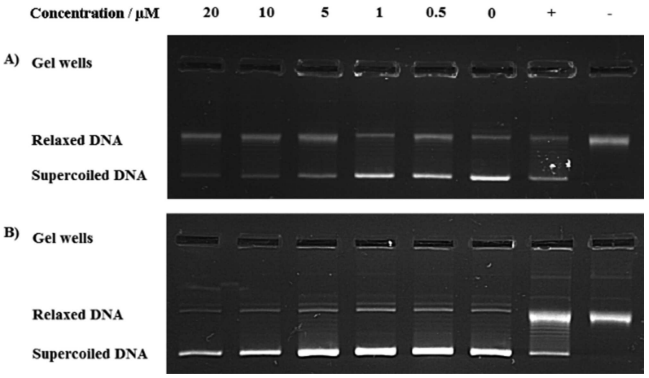

Figure 13. DNA gyrase assay of (A) ciprofloxacin and (B) conjugate **1**. 0 μM = DMSO control. + = positive control, with DNA gyrase present without the antimicrobial. − = negative control, no DNA gyrase or antimicrobial.

intracellular drug target DNA gyrase by **1** was detectable at concentrations of 30 μM and above, with complete inhibition at 75 μM (Figure 14), indicating a decrease in gyrase

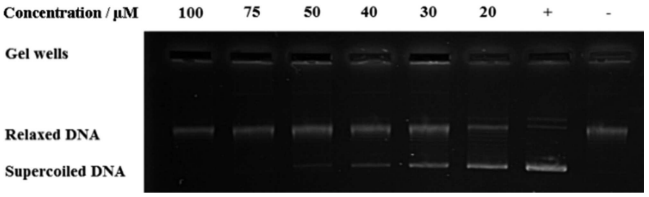

Figure 14. DNA gyrase assay of conjugate **1** at concentrations ranging from 100 to 20 μM.

inhibitory activity in comparison with the parent drug (10 μM). However, this moderate decrease in gyrase inhibitory activity does not explain the drastic drop in the antibacterial potency of **1**.

This, plus the lack of higher activity vs the Nissle 1917 strain, suggests that poor active transport of **1** is a major factor in the observed lack of antimicrobial activity against both strains of *E. coli*.

SUMMARY AND CONCLUSIONS

A ciprofloxacin siderophore conjugate **1** has been synthesized by linking glycosylated catechol units **7**, found in salmochelin S4, to L-lysine modified ciprofloxacin **10**. The resulting siderophore−ciprofloxacin conjugate was designed to evade the mammalian immune response and to selectively target pathogenic bacteria that express the salmochelin receptor IroN. Initial screening of **1** against a common laboratory strain of *E. coli* lacking the IroN transporter demonstrated much reduced antibacterial activity compared to the parent antibiotic ciprofloxacin, with concentrations *ca.* 250−1000× higher than required to obtain similar activity in identical conditions. Increased antibacterial activity was observed in iron deplete media. Probing cellular uptake *via* ^{67}Ga labeling suggested the absence of significant bacterial cell uptake of ^{67}Ga-**1**, consistent with the absence of IroN.

When the activity was examined vs Nissle 1917, a strain capable of expressing IroN, a similar concentration dependence was observed, with **1** again requiring concentrations 250−1000× higher than ciprofloxacin to obtain similar growth inhibition, suggesting the presence of IroN did not lead to significantly greater uptake. Again, higher activity was observed in iron deplete media.

While the DNA gyrase inhibitory activity of **1** was significantly lower than that of the parent drug, the relatively moderate decrease in gyrase inhibitory activity does not explain the drastic drop in the antibacterial potency of **1**.

These results suggest that one major obstacle in the successful application of salmochelin-based Trojan Horse antibiotics with an intracellular drug target is the delivery of the conjugate into the bacterial cell *via* Fe^{3+}-siderophore transporters.

The observed formation of dimeric 2:2 species by native mass spectrometry provides a potential explanation for the observed lack of cellular uptake of conjugate **1**. If the tendency to form dimers also applies to biological media, it is unlikely that these dimers would be recognized by the outer membrane receptor IroN and fit through the iron−salmochelin transporter.

Hence, our first generation conjugate, **1**, the tetradentate mimic of the hexadentate siderophore salmochelin S4, appears poorly suited to target the salmochelin-mediated uptake pathway. A similar relationship was observed for enterobactin−ciprofloxacin Trojan Horse conjugates by Nolan and co-workers,[18] who observed that an intact hexadentate enterobactin unit was required for good antibacterial activity, whereas tetradentate or bidentate equivalents displayed poor activity, possibly due to reduced recognition by the corresponding outer membrane receptor.[18] It is also conceivable that the lack of a flexible linker between the siderophore component and ciprofloxacin renders **1** too rigid and bulky to be able to pass through the IroN transporter or the closely linked ciprofloxacin directly impedes siderophore binding.

The poor cellular uptake shown in the case of **1**, along with its increase in activity in iron deplete media, may point to extracellular Fe^{3+} sequestration as an additional mechanism of action, alongside DNA gyrase inhibition.

While the lack of significant uptake and activity of **1** is disappointing, it offers some direction to a future second generation design. The size and polar surface area of the conjugate are sufficient to prevent passive uptake *via* porin channels or passive diffusion through the cell membrane, suggesting that optimization of the siderophore component and linker to boost uptake in salmochelin-utilizing strains could be sufficient to transform similar conjugates into narrow-spectrum antimicrobials. In addition, while the application of a biolabile linker designed to cleave the ciprofloxacin from the siderophore inside the cell could retrieve the DNA inhibitory activity, a biolabile link will not increase antibiotic efficacy unless the conjugate is delivered, at an appropriate level, into the bacterial cytoplasm. Future studies will be focused on optimizing active conjugate transport into bacterial cells using a combination of targeted chemical synthesis and radiolabeled ^{67}Ga complex uptake studies.

https://dx.doi.org/10.1021/acsinfecdis.0c00568
ACS Infect. Dis. 2020, 6, 2532−2541

■ ASSOCIATED CONTENT

Supporting Information

The Supporting Information is available free of charge at https://pubs.acs.org/doi/10.1021/acsinfecdis.0c00568.

Full experimental details and screening methodology (PDF)

■ AUTHOR INFORMATION

Corresponding Authors

Anne Routledge − *Department of Chemistry, University of York, York YO10 5DD, United Kingdom*; Phone: +44 (0) 1904 322501; Email: anne.routledge@york.ac.uk; Fax: +44 (0) 1904 322516

Anne-Kathrin Duhme-Klair − *Department of Chemistry, University of York, York YO10 5DD, United Kingdom*; orcid.org/0000-0001-6214-2459; Phone: +44 (0) 1904 322587; Email: anne.duhme-klair@york.ac.uk; Fax: +44 (0) 1904 322516

Eszter Boros − *Department of Chemistry, Stony Brook University, Stony Brook, New York 11790, United States*; orcid.org/0000-0002-4186-6586; Phone: (631) 632-8572; Email: eszter.boros@stonybrook.edu

Authors

Thomas J. Sanderson − *Department of Chemistry, University of York, York YO10 5DD, United Kingdom*

Conor M. Black − *Department of Chemistry, University of York, York YO10 5DD, United Kingdom*

James W. Southwell − *Department of Chemistry, University of York, York YO10 5DD, United Kingdom*

Ellis J. Wilde − *Department of Chemistry, University of York, York YO10 5DD, United Kingdom*

Apurva Pandey − *Department of Chemistry, Stony Brook University, Stony Brook, New York 11790, United States*

Reyme Herman − *Department of Biology (Area 10), University of York, York YO10 5DD, United Kingdom*

Gavin H. Thomas − *Department of Biology (Area 10), University of York, York YO10 5DD, United Kingdom*; orcid.org/0000-0002-9763-1313

Complete contact information is available at: https://pubs.acs.org/10.1021/acsinfecdis.0c00568

Author Contributions

A.-K.D.-K., A.R., J.W.S., G.H.T., and E.B. conceived and designed the experiments. T.J.S., C.M.B., J.W.S., E.J.W., A.P., and R.H. performed the experiments. A.-K.D.-K., A.R., C.M.B., J.W.S., and E.B. cowrote the manuscript.

Notes

The authors declare no competing financial interest.

■ ACKNOWLEDGMENTS

A-K.D.-K. and A.R. would like to thank the UK Engineering and Physical Sciences Research Council (EPSRC) for studentships for T.J.S. (EP/K503216/1), E.J.W. (EP/L505122/1), and C.M.B. (EP/N509802/1) and the University of York, Department of Chemistry, for a Teaching Studentship for J.W.S. A.-K.D.-K. acknowledges EPSRC grants EP/T007338/1 and EP/L024829/1. A.-K.D.-K. and A.R. thank J. E. Thomas-Oates for helpful discussions, K. Heaton and H. Robinson for acquisition of mass spectrometry data, P. Aguiar, B. Coulson, and H. Fish for NMR experiments, and G. McAllister for elemental analyses. A.P. and E.B. acknowledge Dr. Peter Tonge for access to the *E. coli* MG1655 strain.

■ REFERENCES

(1) Davies, S. C, Fowler, T., Watson, J., Livermore, D. M, and Walker, D. (2013) Annual Report of the Chief Medical Officer: Infection and the rise of antimicrobial resistance. *Lancet 381*, 1606−1609.

(2) WHO (2014) *Antimicrobial resistance: global report on surveillance*, World Heath Organization, Geneva.

(3) O'Neill, J. (2016) *Tackling Drug-Resistant Infections Globally: Final Report and Recommendations*, The Review on Antimicrobial Resistance, https://amr-review.org/home.html (accessed 2020-01-06).

(4) WHO (2017) *Antibacterial Agents in Clinical Development*, World Health Organization, Geneva.

(5) Mislin, G. L. A., and Schalk, I. J. (2014) Siderophore-dependent iron uptake systems as gates for antibiotic Trojan Horse strategies against Pseudomonas aeruginosa. *Metallomics 6*, 408−420.

(6) Chellat, M. F., Raguz, L., and Riedl, R. (2016) Targeting antibiotic resistance. *Angew. Chem., Int. Ed. 55*, 6600−6626.

(7) Pew Charitable Trusts (2016) *A Scientific Roadmap for Antibiotic Discovery*, https://www.pewtrusts.org/en/research-and-analysis/reports/2016/05/a-scientific-roadmap-for-antibiotic-discovery.

(8) González-Bello, C. (2017) Antibiotic adjuvants - A strategy to unlock bacterial resistance. *Bioorg. Med. Chem. Lett. 27*, 4221−4228.

(9) Miller, M. J., and Malouin, F. (1993) Microbial iron chelators as drug delivery agents: the rational design and synthesis of siderophore-drug conjugates. *Acc. Chem. Res. 26* (5), 241−249.

(10) Stojiljkovic, I., Kumar, V., and Srinivasan, N. (1999) Non-iron metalloporphyrins: potent antibacterial compounds that exploit haem/Hb uptake systems of pathogenic bacteria. *Mol. Microbiol. 31* (2), 429−442.

(11) Roosenberg II, J. M., Lin, Y.-M., Lu, Y., and Miller, M. J. (2000) Studies and syntheses of siderophores, microbial iron chelators, and analogs as potential drug delivery agents. *Curr. Med. Chem. 7*, 159−197.

(12) Tillotson, G. S. (2016) Trojan Horse antibiotics - A novel way to circumvent Gram-negative bacterial resistance? *Infect. Dis.: Res. Treat. 9*, 45−52.

(13) Klahn, P., and Brönstrup, M. (2017) Bifunctional antimicrobial conjugates and hybrid antimicrobials. *Nat. Prod. Rep. 34*, 832−885.

(14) Tan, L., Tao, Y., Wang, T., Zou, F., Zhang, S., Kou, Q., Niu, A., Chen, Q., Chu, W., Chen, X., Wang, H., and Yang, Y. (2017) Discovery of novel pyridone-conjugated monosulfactams as potent and broad-spectrum antibiotics for multidrug-resistant Gram-negative infections. *J. Med. Chem. 60*, 2669−2684.

(15) Ferreira, K., Hu, H.-Y., Fetz, V., Prochnow, H., Rais, B., Müller, P. P., and Brönstrup, M. (2017) Multivalent siderophore-DOTAM conjugates as theranostics for imaging and treatment of bacterial infections. *Angew. Chem., Int. Ed. 56* (28), 8272−8276.

(16) Ghosh, M., Miller, P. A., Möllmann, U., Claypool, W. D., Schroeder, V. A., Wolter, W. R., Suckow, M., Yu, H., Li, S., Huang, W., Zajicek, J., and Miller, M. J. (2017) Targeted antibiotic delivery: selective siderophore conjugation with daptomycin confers potent activity against multidrug resistant Acinetobacter baumannii both in vitro and in vivo. *J. Med. Chem. 60*, 4577−4583.

(17) Liu, R., Miller, P. A., Vakulenko, S. B., Stewart, N. K., Boggess, W. C., and Miller, M. J. (2018) A synthetic dual drug sideromycin induces gram-negative bacteria to commit suicide with a gram-positive antibiotic. *J. Med. Chem. 61*, 3845−3854.

(18) Neumann, W., Sassone-Corsi, M., Raffatellu, M., and Nolan, E. M. (2018) Esterase-catalyzed siderophore hydrolysis activates an enterobactin-ciprofloxacin conjugate and confers targeted antibacterial activity. *J. Am. Chem. Soc. 140* (15), 5193−5201.

(19) Pandey, A., Savino, C., Ahn, S. H., Yang, Z., Van Lanen, S. G., and Boros, E. (2019) Theranostic gallium siderophore ciprofloxacin conjugate with broad spectrum antibiotic potency. *J. Med. Chem. 62* (21), 9947−9960.

(20) Negash, K. H., Norris, J. K. S., and Hodgkinson, J. T. (2019) Siderophore-antibiotic conjugate design: New drugs for bad bugs? *Molecules 24*, 3314−3330.
(21) To the best of our knowledge, at least four siderophore-based Trojan Horse antibiotics have entered clinical trials: cefiderocol (S-649266), GSK-3342830, cefetecol, and BAL-30072 (see refs 4, 22, and 23). A number of others have failed at the preclinical stage.
(22) Butler, M. S., Blaskovich, M. A., and Cooper, M. A. (2013) Antibiotics in the clinical pipeline in 2013. *J. Antibiot. 66*, 571−591.
(23) Page, M. G. P. (2019) The role of iron and siderophores in infection, and the development of siderophore antibiotics. *Clin. Infect. Dis. 69* (Supplement 7), S529−S537.
(24) FDA (2019) *FDA approves new antibacterial drug to treat complicated urinary tract infections as part of ongoing efforts to address antimicrobial resistance*, https://www.fda.gov/news-events/press-announcements/fda-approves-new-antibacterial-drug-treat-complicated-urinary-tract-infections-part-ongoing-efforts (accessed 2020-01-07).
(25) Hantke, K., Nicholson, G., Rabsch, W., and Winkelmann, G. (2003) Salmochelins, siderophores of Salmonella enterica and uropathogenic Escherichia coli strains, are recognized by the outer membrane receptor IroN. *Proc. Natl. Acad. Sci. U. S. A. 100* (7), 3677−3682.
(26) Fiedler, H.-P., Krastel, P., Müller, J., Gebhardt, K., and Zeeck, A. (2001) Enterobactin: the characteristic catecholate siderophore of Enterobacteriaceae is produced by Streptomyces species. *FEMS Microbiol. Lett. 196* (2), 147−151.
(27) Bister, B., Bischoff, D., Nicholson, G. J., Valdebenito, M., Schneider, K., Winkelmann, G., Hantke, K., and Süssmuth, R. D. (2004) The structure of salmochelins: C-glucosylated enterobactins of Salmonella enterica. *BioMetals 17*, 471−481.
(28) Valdebenito, M., Bister, B., Reissbrodt, R., Hantke, K., and Winkelmann, G. (2005) The detection of salmochelin and yersiniabactin in uropathogenic Escherichia coli strains by a novel hydrolysis-fluorescence-detection (HFD) method. *Int. J. Med. Microbiol. 295*, 99−107.
(29) Valdebenito, M., Crumbliss, A. L., Winkelmann, G., and Hantke, K. (2006) Environmental factors influence the production of enterobactin, salmochelin, aerobactin, and yersiniabactin in *Escherichia coli* strain Nissle 1917. *Int. J. Med. Microbiol. 296* (8), 513−520.
(30) Fischbach, M. A., Lin, H., Zhou, L., Yu, Y., Abergel, R. J., Liu, D. R., Raymond, K. N., Wanner, B. L., Strong, R. K., Walsh, C. T., Aderem, A., and Smith, K. D. (2006) The pathogen-associated iroA gene cluster mediates bacterial evasion of lipocalin 2. *Proc. Natl. Acad. Sci. U. S. A. 103* (44), 16502−16507.
(31) Goetz, D. H., Holmes, M. A., Borregaard, N., Bluhm, M. E., Raymond, K. N., and Strong, R. K. (2002) The neutrophil lipocalin NGAL is a bacteriostatic agent that interferes with siderophore-mediated iron acquisition. *Mol. Cell 10*, 1033−1043.
(32) Flo, T. H., Smith, K. D., Sato, S., Rodriguez, D. J., Holmes, M. A., Strong, R. K., Akira, S., and Aderem, A. (2004) Lipocalin 2 mediates an innate immune response to bacterial infection by sequestrating iron. *Nature 432*, 917−921.
(33) Müller, S. I., Valdebenito, M., and Hantke, K. (2009) Salmochelin, the long-overlooked catecholate siderophore of Salmonella. *BioMetals 22*, 691−695.
(34) Zhu, M., Valdebenito, M., Winkelmann, G., and Hantke, K. (2005) Functions of the siderophore esterases IroD and IroE in iron-salmochelin utilization. *Microbiology 151* (7), 2363−2372.
(35) Crouch, M-L. V., Castor, M., Karlinsey, J. E., Kalhorn, T., and Fang, F. C. (2008) Biosynthesis and IroC-dependent export of the siderophore salmochelin are essential for virulence of *Salmonella enterica* serovar Typhimurium. *Mol. Microbiol. 67* (5), 971−983.
(36) Raymond, K. N., Dertz, E. A., and Kim, S. S. (2003) Enterobactin: An archetype for microbial iron transport. *Proc. Natl. Acad. Sci. U. S. A. 100* (7), 3584−3588.
(37) Andrews, S. C., Robinson, A. K., and Rodríguez-Quiñones, F. (2003) Bacterial iron homeostasis. *FEMS Microbiol. Rev. 27*, 215−237.
(38) Krewulak, K. D., and Vogel, H. J. (2008) Structural biology of bacterial iron uptake. *Biochim. Biophys. Acta, Biomembr. 1778* (9), 1781−1804.
(39) Chairatana, P., Zheng, T., and Nolan, E. M. (2015) Targeting virulence: salmochelin modification tunes the antibacterial activity spectrum of β-lactams for pathogen-selective killing of *Escherichia coli*. *Chem. Sci. 6*, 4458−4471.
(40) Md-Saleh, S. R., Chilvers, E. C., Kerr, K. G., Milner, S. J., Snelling, A. M., Weber, J. P., Thomas, G. H., Duhme-Klair, A.-K., and Routledge, A. (2009) Synthesis of citrate-ciprofloxacin conjugates. *Bioorg. Med. Chem. Lett. 19*, 1496−1498.
(41) Milner, S. J., Seve, A., Snelling, A. M., Thomas, G. H., Kerr, K. G., Routledge, A., and Duhme-Klair, A.-K. (2013) Staphyloferrin A as siderophore-component in fluoroquinolone-based Trojan Horse antibiotics. *Org. Biomol. Chem. 11*, 3461−3468.
(42) Milner, S. J., Snelling, A. M., Kerr, K. G., Abd-El-Aziz, A., Thomas, G. H., Hubbard, R. E., Routledge, A., and Duhme-Klair, A.-K. (2014) Probing linker design in citric acid-ciprofloxacin conjugates. *Bioorg. Med. Chem. 22*, 4499−4505.
(43) Heinisch, L., Wittmann, S., Stoiber, T., Berg, A., Ankel-Fuchs, D., and Möllmann, U. (2002) Highly antibacterial active aminoacyl penicillin conjugates with acylated bis-catecholate siderophores based on secondary diamino acids and related compounds. *J. Med. Chem. 45* (14), 3032−3040.
(44) Möllmann, U., Heinisch, L., Bauernfeind, A., Köhler, T., and Ankel-Fuchs, D. (2009) Siderophores as drug delivery agents: application of "Trojan Horse" strategy. *BioMetals 22*, 615−624.
(45) Raines, D. J., Moroz, O. V., Blagova, E. V., Turkenburg, J. P., Wilson, K. S., and Duhme-Klair, A.-K. (2016) Bacteria in an intense competition for iron: key component of the Campylobacter jejuni iron uptake system scavenges enterobactin hydrolysis product. *Proc. Natl. Acad. Sci. U. S. A. 113*, 5850−5855.
(46) Wilde, E. J., Blagova, E. V., Sanderson, T. J., Raines, D. J., Thomas, R. P., Routledge, A., Duhme-Klair, A.-K., and Wilson, K. S. (2019) Mimicking salmochelin S1 and the interactions of its Fe(III) complex with periplasmic iron siderophore binding proteins CeuE and VctP. *J. Inorg. Biochem. 190*, 75−84.
(47) Turel, I. (2002) The interactions of metal ions with quinolone antibacterial agents. *Coord. Chem. Rev. 232* (1−2), 27−47.
(48) Uivarosi, V. (2013) Metal complexes of quinolone antibiotics and their applications: an update. *Molecules 18* (9), 11153−11197.
(49) Joshua, A. V., Sharma, S. K., and Abrams, D. N. (2008) New short synthesis of (5)-2,3-dimethoxy-N-[(1-ethyl-2-pyrrolidinyl)-methyl]-5-iodobenzamide: dopamine D2 receptor. *Synth. Commun. 38*, 434−440.
(50) Gong, H. G., and Gagné, M. R. (2008) Diastereoselective Ni-catalyzed Negishi cross-coupling approach to saturated, fully oxygenated C-alkyl and C-aryl glycosides. *J. Am. Chem. Soc. 130*, 12177−12183.
(51) Yu, X. L., Dai, Y. J., Yang, T., Gagné, M. R., and Gong, H. G. (2011) Facile synthesis of salmochelin S1, S2, MGE, DGE, and TGE. *Tetrahedron 67*, 144−151.
(52) Pearlman, W. M. (1967) Noble metal hydroxides on carbon nonpyrophoric dry catalysts. *Tetrahedron Lett. 8*, 1663−1664.
(53) Hirai, K., Aoyama, H., Suzue, S., Irikura, T., Iyobe, S., and Mitsuhashi, S. (1986) Isolation and characterization of norfloxacin-resistant mutants of *Escherichia coli* K-12. *Antimicrob. Agents Chemother. 30*, 248−253.
(54) Neves, P., Berkane, E., Gameiro, P., Winterhalter, M., and de Castro, B. (2005) Interaction between quinolones antibiotics and bacterial outer membrane porin OmpF. *Biophys. Chem. 113*, 123−128.
(55) Low, A. S., MacKenzie, F. M., Gould, I. M., and Booth, I. R. (2001) Protected environments allow parallel evolution of a bacterial pathogen in a patient subjected to long-term antibiotic therapy. *Mol. Microbiol. 42* (3), 619−630.
(56) Vinué, L., Corcoran, M. A., Hooper, D. C., and Jacoby, G. A. (2016) Mutations that enhance the ciprofloxacin resistance of *Escherichia coli* with qnrA1. *Antimicrob. Agents Chemother. 60* (3), 1537−1545.

https://dx.doi.org/10.1021/acsinfecdis.0c00568
ACS Infect. Dis. 2020, 6, 2532−2541

(57) Prajapati, J. D., Solano, C. J. F., Winterhalter, M., and Kleinekathöfer, U. (2017) Characterization of ciprofloxacin permeation pathways across the porin OmpC using metadynamics and a string method. *J. Chem. Theory Comput. 13*, 4553−4566.
(58) Nikaido, H. (1994) Porins and specific diffusion channels in bacterial outer membranes. *J. Biol. Chem. 269* (6), 3905−3908.
(59) Delcour, A. H. (2009) Outer membrane permeability and antibiotic resistance. *Biochim. Biophys. Acta, Proteins Proteomics 1794*, 808−816.
(60) Colomer, I., Empson, C. J., Craven, P., Owen, Z., Doveston, R. G., Churcher, I., Marsden, S. P., and Nelson, A. (2016) A divergent synthetic approach to diverse molecular scaffolds: assessment of lead-likeness using LLAMA, an open-access computational tool. *Chem. Commun. 52*, 7209−7212.
(61) Palm, K., Sternberg, P., Luthman, K., and Artursson, P. (1997) Polar molecular surface properties predict the intestinal absorption of drugs in humans. *Pharm. Res. 14*, 568−571.
(62) Neidhardt, F. C., Bloch, P. L., and Smith, D. F. (1974) Culture medium for Enterobacteria. *J. Bacteriol. 119* (3), 736−747.
(63) Emery, T., and Hoffer, P. B. (1980) Siderophore-mediated mechanism of gallium uptake demonstrated in the microorganism Ustilago sphaerogena. *J. Nucl. Med. 21*, 935−939.
(64) Clarke, T. E., Braun, V., Winkelmann, G., Tari, L. W., and Vogel, J. H. (2002) X-ray crystallographic structures of the *Escherichia coli* periplasmic protein FhuD bound to hydroxamate-type siderophores and the antibiotic albomycin. *J. Biol. Chem. 277*, 13966−13972.
(65) Kelson, A. B., Carnevali, M., and Truong-Le, V. (2013) Gallium-based anti-infectives: targeting microbial iron-uptake mechanisms. *Curr. Opin. Pharmacol. 13*, 707−716.
(66) Petrik, M., Haas, H., Dobrozemsky, G., Lass-Flörl, C., Helbok, A., Blatzer, M., Dietrich, H., and Decristoforo, C. (2010) ^{68}Ga-Siderophores for PET imaging of invasive pulmonary aspergillosis: proof of principle. *J. Nucl. Med. 51* (4), 639−645.
(67) Beasley, F. C., and Heinrichs, D. E. (2010) Siderophore-mediated iron acquisition in the staphylococci. *J. Inorg. Biochem. 104* (3), 282−288.
(68) Ioppolo, J. A., Caldwell, D., Beiraghi, O., Llano, L., Blacker, M., Valliant, J. F., and Berti, P. J. (2017) ^{67}Ga-labeled deferoxamine derivatives for imaging bacterial infection: Preparation and screening of functionalized siderophore complexes. *Nucl. Med. Biol. 52*, 32−41.
(69) Balbontín, R., Villagra, N., de la Gándara, M. P., Mora, G., Figueroa-Bossi, N., and Bossi, L. (2016) Expression of IroN, the salmochelin siderophore receptor requires mRNA activation by RyhB small RNA homologues. *Mol. Microbiol. 100* (1), 139−155.

https://dx.doi.org/10.1021/acsinfecdis.0c00568
ACS Infect. Dis. 2020, 6, 2532−2541